

## ***UV-C irradiation is highly effective in inactivating and inhibiting SARS-CoV-2 replication***

Andrea Bianco<sup>1,§</sup>, Mara Biasin<sup>2,§</sup>, Giovanni Pareschi<sup>1</sup>, Adalberto Cavalieri<sup>3</sup>, Claudia Cavatorta<sup>3</sup>, Claudio Fenizia<sup>2</sup>, Paola Galli<sup>1</sup>, Luigi Lessio<sup>4</sup>, Manuela Lualdi<sup>3</sup>, Edoardo Redaelli<sup>1</sup>, Irma Saulle<sup>2,5</sup>, Daria Trabattoni<sup>2</sup>, Alessio Zanutta<sup>1</sup>, Mario Clerici<sup>5,6,\*</sup>

<sup>1</sup> Italian National Institute for Astrophysics (INAF) – Brera Astronomical Observatory, Milano/Merate, Italy.

<sup>2</sup> Department of Biomedical and Clinical Sciences L. Sacco, University of Milano, Milano, Italy.

<sup>3</sup> Department of Imaging Diagnostic and Radioterapy, IRCCS Foundation, Istituto Nazionale dei Tumori, Milan, Italy.

<sup>4</sup> Italian National Institute for Astrophysics (INAF) – Padova Astronomical Observatory, Padova, Italy.

<sup>5</sup> Department of Pathophysiology and Transplantation, University of Milano, Milano, Italy.

<sup>6</sup> Don C. Gnocchi Foundation, IRCCS Foundation, Milano, Italy.

***The potential virucidal effects of UV-C irradiation on SARS-CoV-2 were experimentally evaluated for different illumination doses and virus concentrations (1000, 5, 0.05 MOI). Both virus inactivation and replication inhibition were investigated as a function of these parameters. At a virus density comparable to that observed in SARS-CoV-2 infection, an UV-C dose of just 3.7 mJ/cm<sup>2</sup> was sufficient to achieve a 3-log inactivation, and complete inhibition of all viral concentrations was observed with 16.9 mJ/cm<sup>2</sup>. These results could explain the epidemiological trends of COVID-19 and are important for the development of novel sterilizing methods to contain SARS-CoV-2 infection.***

The COVID-19 pandemic caused by SARS-CoV-2 virus<sup>1</sup> has had an enormous, as yet barely understood, impact on health and economic outlook at the global level<sup>2</sup>. The identification of effective microbicide approaches is of paramount importance in order to limit further viral spread, as the virus can be transmitted via aerosol<sup>3</sup> and can survive for hours outside the body<sup>4</sup>. In this context, non-contact disinfection technologies are highly desirable, and UV radiation, in particular UV-C (200 – 280 nm), is one of the most reliable and widely accepted approach<sup>5–8</sup>. The interaction of UV-C radiations with viruses has been extensively studied<sup>9</sup>, and the most common mechanism consists in direct absorption of the UV-C photon by the nucleic acid basis and/or capsid proteins leading to the generation of photoproducts that inactivate the virus<sup>10,11</sup>. Some models have been proposed to correlate the nucleic acid structure with the required dose to inactivate the virus, but we are far from a reliable model<sup>12</sup>. This is also due to the fact that UV-C measurements were conducted using different viruses and diverse experimental conditions<sup>13–16</sup>. This led to an extremely wide range of values for the same virus and, e.g. in the case of SARS-COV-1 values reported in the literature range from a few mJ/cm<sup>2</sup> to hundreds mJ/cm<sup>2</sup><sup>13,16,17</sup>. It is therefore crucial to have direct

**NOTE: This preprint reports new research that has not been certified by peer review and should not be used to guide clinical practice.**

evidences of UV-C disinfection mechanism on SARS-CoV-2 with the corresponding doses, knowing that the UV light from sunlight seems to be efficient in inactivating the virus<sup>18</sup>.

Herein, we report the effect of monochromatic UV-C (254 nm) on SARS-CoV-2, showing that both virus inactivation and inhibition can be easily achieved. Experiments were conducted using a custom-designed low-pressure mercury lamp system, which has been spectral-calibrated providing an average intensity of 1.082 mW/cm<sup>2</sup> over the illumination area (see the supplementary information for the details). Three different illumination exposure times, corresponding to 3.7, 16.9 and 84.4 mJ/cm<sup>2</sup>, were administered to SARS-CoV-2 either at a multiplicity of infection (MOI) of 0.05, 5, 1000. The first concentration is equivalent to the low-level contamination observed in closed environments (e.g. hospital rooms), the second one corresponds to the average concentration found in the sputum of COVID-19 infected patients, and the third one is a very large concentration, corresponding to that observed in terminally diseased COVID-19 patients<sup>19</sup>. After exposure to UV-C, viral replication<sup>19</sup> was assessed by Real Time Polymerase Chain Reaction (PCR) targeting two regions (N1 and N2) of the SARS-CoV-2 nucleocapsid gene, as well as by analyzing SARS-CoV-2-induced cytopathic effect. Analyses were performed in the culture supernatant of infected cells at three different time points (24, 48 and 72 hours for SARS-CoV-2 at MOI 1000 and 5; 24, 48 hours and 6 days for SARS-CoV-2 at MOI 0.05) as well as on cell lysates at the end of cellular culture (72 hours: MOI 1000 and 5; 6 days: MOI 0.05).

The effect of the UV-C exposure was extremely evident independently from the MOI employed; dose-response and a time-dependent curves were observed. Figure 1 reports the number of SARS-CoV-2 copies for the three concentrations as a function of the UV-C dose and time, quantified on a standard curve from a plasmid control.

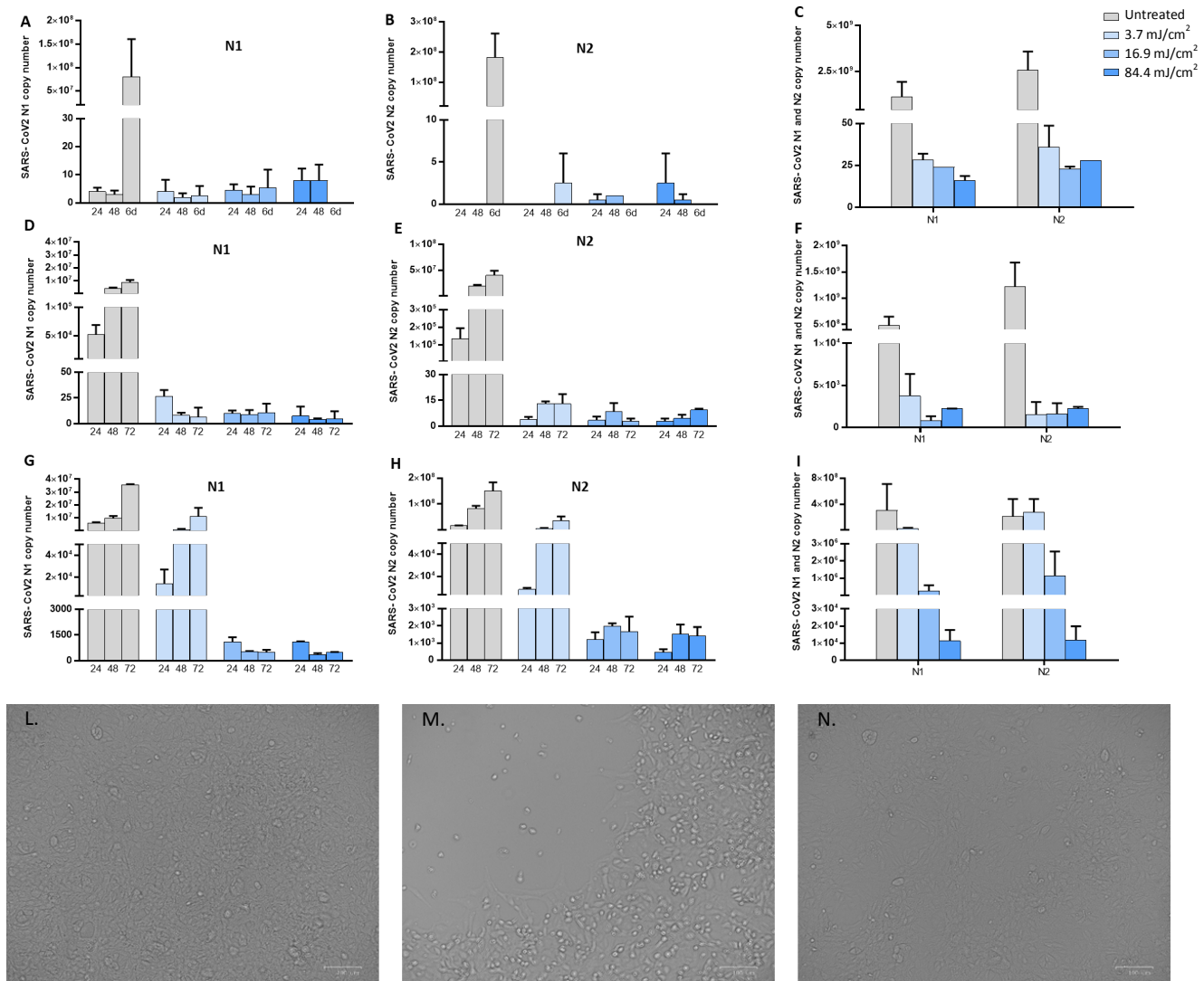


Figure 1. Viral replication of UV-irradiated SARS-CoV-2 virus in in vitro VeroE6 cells. Vero E6 cells were infected with UV-C irradiated SARS-CoV-2 virus at a MOI of 0.05 (A, B and C), 5 (D, E and F) or 1000 (G, H and I). Culture supernatants were harvested at the indicated times (24, 48 72 hours and 6 days) and virus titers were measured by absolute copy number quantification (Real-Time PCR) (A, B, D, E, G and F). Viral replication was assessed on cell lysate harvested at the end of cell cultures at 72 hours (5 and 1000 MOI) (panel F and I) and 6 days (0,05 MOI) (Panel C) post infection. All cell culture conditions were seeded in duplicate. (L) No cytopathic effect was observed in uninfected cultured VeroE6 monolayers maintained in 50mJ/cm<sup>2</sup> UV-treated complete medium for 72 hours. (M) In vitro infection of SARS-CoV-2 (5 MOI) UV-C untreated VeroE6 cells resulted in an evident cytopathic effect. (N) SARS-CoV-2 irradiation with 3.7 mJ/cm<sup>2</sup> UV-C rescued the cytopathic effect induced by UV-C untreated virus.

Viral replication could not be observed for the first 48 hours at the lowest concentration (0.05 MOI) in either untreated or UV-C-irradiated samples. However, 6 days after infection viral replication was distinctly

evident in the UV-C unexposed condition, but was completely inhibited following UV-C irradiation even at 3.7 mJ/cm<sup>2</sup> in both cell culture supernatants (Figure 1, panel A and B) and cell lysate (Figure 1, panel C). At the intermediate viral concentration (5 MOI), an effective reduction of copy number starting from the 3.7 mJ/cm<sup>2</sup> dose with a decrease of a factor of 2000 (> 3-log decrease) after 24 hours (Figure 1, panel D) was observed. Even more important, the copy number value did not increase over time, suggesting an effective inactivation of the virus, further confirmed by cytopathic effect assessment (Figure 1, panel L, M and N). The highest UV-C doses followed the same trend (Figure 1, panel D and E). Evaluation of viral replication at intracellular level further corroborated the antiviral UV-C effect (Figure 1, panel F). Therefore, at this viral input exposure to a minimal dose of 3.7 mJ/cm<sup>2</sup> result in viral depletion.

The outcome was different with the highest viral input (1000 MOI). Indeed, viral replication significantly decreased in a UV-C dose-dependent manner as early as 24 hours with a factor of 10<sup>3</sup> at 3.7 mJ/cm<sup>2</sup> and 5x10<sup>5</sup> at 16.9 mJ/cm<sup>2</sup>. After 48 hours, viral concentration increased in cultures exposed to the lowest UV-C dose, whereas it remained stable for the 16.9 and 84.4 mJ/cm<sup>2</sup> doses, consistent with the results at 72 hours (Figure 1, panel G and H). Results were confirmed by assessment of viral replication at intracellular level (Figure 1, panel I). This clearly indicates that the residual viral input left by the 3.7 mJ/cm<sup>2</sup> was able to replicate and enough to generate an effective infection. Therefore, the partial inactivation of the viral input led to an inhibition of infection. This is not the case in cultures exposed to higher UV-C doses, as no replication could be detected in these conditions.

In conclusion, UV-C radiation inhibit SARS-CoV-2 and the response depends on both the UV-C dose and the virus concentration. Indeed, for virus concentrations typical of low-level contaminated closed environment and sputum of COVID-19 infected patients, a very small dose of less than 4 mJ/cm<sup>2</sup> was enough to achieve full inactivation of the virus. Even at the highest viral input concentration (1000 MOI), viral replication was totally inactivated at a dose  $\geq 16.9$  mJ/cm<sup>2</sup>. These results are extremely important since they allow for a proper design and development of efficient UV based disinfection methods to contain SARS-CoV-2 infection.

## Acknowledgements

This research was partially supported by a grant from Falk Renewables and it has been carried out in the context of the activities promoted by the Italian Government and in particular, by the Ministries of Health and of University and Research, against the COVID-19 pandemic. Authors are grateful to INAF's President, Prof. N. D'Amico, for the support and for a critical reading of the manuscript.

## References

1. Zhu, N. *et al.* A Novel Coronavirus from Patients with Pneumonia in China, 2019. *N. Engl. J. Med.* **382**, 727–733 (2020).
2. Cobey, S. Modeling infectious disease dynamics. *Science*. **368**, 713–714 (2020).
3. van Doremalen, N. *et al.* Aerosol and Surface Stability of SARS-CoV-2 as Compared with SARS-CoV-1. *N. Engl. J. Med.* **382**, 1564–1567 (2020).
4. Stadnytskyi, V., Bax, C. E., Bax, A. & Anfinrud, P. The airborne lifetime of small speech droplets and their potential importance in SARS-CoV-2 transmission. *Proc. Natl. Acad. Sci.* 202006874 (2020) doi:10.1073/pnas.2006874117.
5. Pirnie, M., Linden, K. G. & Malley, J. P. J. Ultraviolet disinfection guidance manual for the final long term 2 enhanced surface water treatment rule. *Environ. Prot.* **2**, 1–436 (2006).
6. Reed, N. G. The history of ultraviolet germicidal irradiation for air disinfection. *Public Health Rep.* **125**, 15–27 (2010).
7. Chang, J. C. *et al.* UV inactivation of pathogenic and indicator microorganisms. *Appl. Environ. Microbiol.* **49**, 1361–1365 (1985).
8. Kovalski, W. *Ultraviolet germicidal irradiation handbook: UVGI for air and surface disinfection*. (Springer Science & Business Media, 2010).
9. Rauth, A. M. The Physical State of Viral Nucleic Acid and the Sensitivity of Viruses to Ultraviolet Light. *Biophys. J.* **5**, 257–273 (1965).
10. Qiao, Z. & Wigginton, K. R. Direct and Indirect Photochemical Reactions in Viral RNA Measured with RT-qPCR and Mass Spectrometry. *Environ. Sci. Technol.* **50**, 13371–13379 (2016).
11. Wigginton, K. R. & Kohn, T. Virus disinfection mechanisms: the role of virus composition, structure, and function. *Curr. Opin. Virol.* **2**, 84–89 (2012).
12. Lytle, C. D. & Sagripanti, J.-L. Predicted Inactivation of Viruses of Relevance to Biodefense by Solar Radiation. *J. Virol.* **79**, 14244–14252 (2005).
13. Walker, C. M. & Ko, G. Effect of Ultraviolet Germicidal Irradiation on Viral Aerosols. *Environ. Sci. Technol.* **41**, 5460–5465 (2007).
14. McDevitt, J. J., Rudnick, S. N. & Radonovich, L. J. Aerosol susceptibility of influenza virus to UV-C light. *Appl. Environ. Microbiol.* **78**, 1666–1669 (2012).
15. Calgua, B. *et al.* UVC Inactivation of dsDNA and ssRNA Viruses in Water: UV Fluences and a qPCR-  
§ These authors contributed equally;\* e-mail: mario.clerici@unimi.it

Based Approach to Evaluate Decay on Viral Infectivity. *Food Environ. Virol.* **6**, 260–268 (2014).

16. Eickmann, M. *et al.* Inactivation of three emerging viruses – severe acute respiratory syndrome coronavirus, Crimean–Congo haemorrhagic fever virus and Nipah virus – in platelet concentrates by ultraviolet C light and in plasma by methylene blue plus visible light. *Vox Sang.* **115**, 146–151 (2020).
17. Duan, S.-M. *et al.* Stability of SARS Coronavirus in Human Specimens and Environment and Its Sensitivity to Heating and UV Irradiation. *Biomed. Environ. Sci.* **16**, 246–255.
18. Ratnesar-Shumate, S. *et al.* Simulated Sunlight Rapidly Inactivates SARS-CoV-2 on Surfaces. *J. Infect. Dis.* 1–9 (2020) doi:10.1093/infdis/jiaa274.
19. Wölfel, R. *et al.* Virological assessment of hospitalized patients with COVID-2019. *Nature* **581**, 465–469 (2020).

## Supplementary information

### ***UV-C irradiation very effectively inactivates and inhibits SARS-CoV-2 replication***

Andrea Bianco<sup>1\*</sup>, Mara Biasin<sup>2\*</sup>, Giovanni Pareschi<sup>3</sup>, Adalberto Cavalieri<sup>4</sup>, Claudia Cavatorta<sup>4</sup>, Claudio Fenizia<sup>5</sup>, Paola Galli<sup>1</sup>, Luigi Lessio<sup>4</sup>, Manuela Lualdi<sup>3</sup>, Edoardo Redaelli<sup>1</sup>, Irma Saulle<sup>2,5</sup>, Daria Trabattoni<sup>2</sup>, Alessio Zanutta<sup>1</sup>, Mario Clerici<sup>5,6</sup>

<sup>1</sup> *Italian National Institute for Astrophysics (INAF) – Brera Astronomical Observatory, Milano/Merate, Italy.*

<sup>2</sup> *Department of Biomedical and Clinical Sciences L. Sacco, University of Milano, Milano, Italy.*

<sup>3</sup> *Department of Imaging Diagnostic and Radioterapy, IRCCS Foundation, Istituto Nazionale dei Tumori, Milan, Italy.*

<sup>4</sup> *Italian National Institute for Astrophysics (INAF) – Padova Astronomical Observatory, Padova, Italy.*

<sup>5</sup> *Department of Pathophysiology and Transplantation, University of Milano, Milano, Italy.*

<sup>6</sup> *Don C. Gnocchi Foundation, IRCCS Foundation, Milano, Italy.*

### ***In vitro SARS-CoV-2 infection assay***

3 x 10<sup>5</sup> VeroE6 cells were cultured in DMEM (Euroclone, Milan, Italy) with 2 % FBS medium, with 100 U/ml penicillin and 100 µg/ml streptomycin, in a 24-well plate one day before viral infection assay. SARS-CoV-2 (Virus Human 2019-nCoV strain 2019- nCoV/Italy-INMI1, Rome, Italy) at a multiplicity of infection (MOI) of 1000, 5 and 0.05 were treated with different doses of UV-C radiation (see the dedicated section) before inoculum into VeroE6 cells. UV-C-untreated virus served as positive controls. Cell cultures were incubated with the virus inoculum in duplicate for three hours at 37°C and 5% CO<sub>2</sub>. Then, cells were rinsed three times with warm PBS, replenished with the appropriate growth medium and observed daily for cytopathic effect. Viral replication in culture supernatants was assessed at 24, 48, and 72 hours post-infection (hpi) while infected cells were harvested for RNA collection at 72 hpi. Cell cultures from SARS-CoV-2 at 0.05 MOI were harvested 6 days post infection. RNA was extracted from VeroE6 cell culture supernatant and cell lysate by the Maxwell<sup>®</sup> RSC Instrument with Maxwell<sup>®</sup> RSC Viral Total Nucleic Acid Purification Kit (Promega, Fitchburg, WI, USA) and retrotranscribed in cDNA as previously described (Promega, Fitchburg, WI, USA). Real-time PCR was performed on a CFX96 (Bio-Rad, CA, USA) using the 2019-nCoV CDC qPCR Probe Assay emergency kit (IDT, Iowa, USA), which targets two regions (N1 and N2) of the nucleocapsid gene of SARS-CoV-2. Viral copy quantification was assessed by creating a standard curve from the quantified 2019-nCoV\_N positive Plasmid Control (IDT, Iowa, USA).

### ***UV illumination test***

The illumination of the virus solution was conducted using a low-pressure mercury lamp mounted in a custom designed holder, which consist in a box with a circular aperture 50 mm in diameter placed at approximately 220 mm from the source. The aperture works as a spatial filter to make the illumination of the area behind more uniform. A mechanical shutter is also present to start the illumination process. The plate is placed 30 mm below the circular aperture and a single dwell (34.7 mm in diameter), centered in respect to the 50 mm aperture, has been irradiated from the top.

The intensity of the lamp and its spectral properties have been measured using an Ocean Optics HR2000+ spectrometer (Ocean Optics Inc., Dunedin, USA). The HR2000+ spectrometer was calibrated against a reference deuterium–halogen source (Ocean Optics Inc. Winter Park, Winter Park, Florida) and in compliance with National Institute of Standards and Technology (NIST) practices recommended in NIST Handbook 150-2E, Technical guide for Optical Radiation Measurements. The last calibration was performed in March 2019. The detector of our spectrometer is a high-sensitivity 2048-element Charge-Coupled Device

(CCD) array from Sony. The spectral range is 200–1100 nm with a 25  $\mu\text{m}$  wide entrance slit and an optical resolution of 1.4 nm (FWHM). The cosine-corrected irradiance probe, model CC-3-UV-T, is attached to the tip of a 1 m long optical fibre and couples to the spectrometer. The intensity of the lamp has been measured by positioning the spectrometer in five positions: in the center and at the ends of a 20 mm cross arm after a warming up time of 30 s. The spectra in the five positions are reported in figure S1 together with a scheme of the dwell and illuminated area.

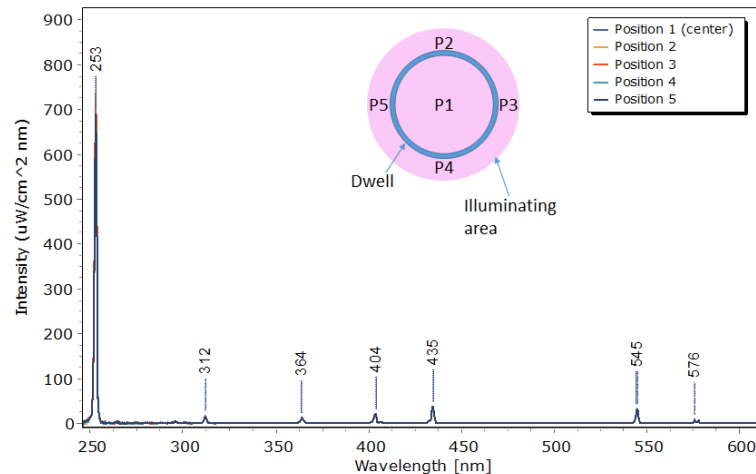


Figure S1. Mercury lamp spectrum measured in the five positions. Inset: scheme of the illuminated dwell and the measuring position.

As expected, the emission is dominated by the UV-C line and its intensity was uniform in the area with an average value of  $1082 \text{ uW/cm}^2$ . The stability of the lamp was evaluated in  $\pm 11 \text{ uW/cm}^2$  during a 130 s measurement. According to this value, three exposure times were set: 5, 23 and 114 s (with an accuracy of 0.2s), which correspond to following doses: 5.5, 25.0,  $124.4 \text{ mJ/cm}^2$ . This is the nominal UV doses provided to the dwell, but we were interested in the effective doses reaching the virus. Therefore, we measured the UV-vis absorption spectrum of the Dulbecco's Modified Eagle's Medium (DMEM) in a quartz cuvette (1 mm thick) by means of a Jasco V770 spectrophotometer (Figure S2). This thickness is the same of the solution in the dwell during the UV irradiation step.

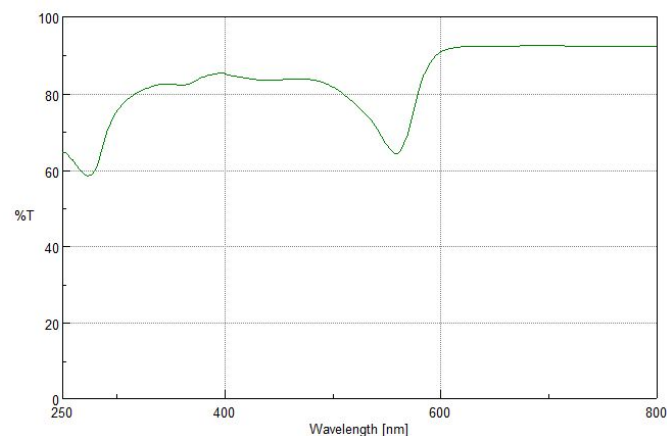


Figure S2. UV-vis transmission spectrum of the Dulbecco's Modified Eagle's Medium (DMEM) in a 1 mm quartz cuvette.

The transmittance at 254 nm has been firstly corrected by the reflection losses of the quartz cuvette; then, the reflection loss due to the air-water interface has been taken into account and a final transmittance of 0.68 at 254 nm was calculated. According to this value, the effective doses provided to the viruses were:  $3.7 \pm 0.15$ ,  $16.9 \pm 0.2$  and  $84.4 \pm 0.9 \text{ mJ/cm}^2$ .



### Plots of the active virus fraction

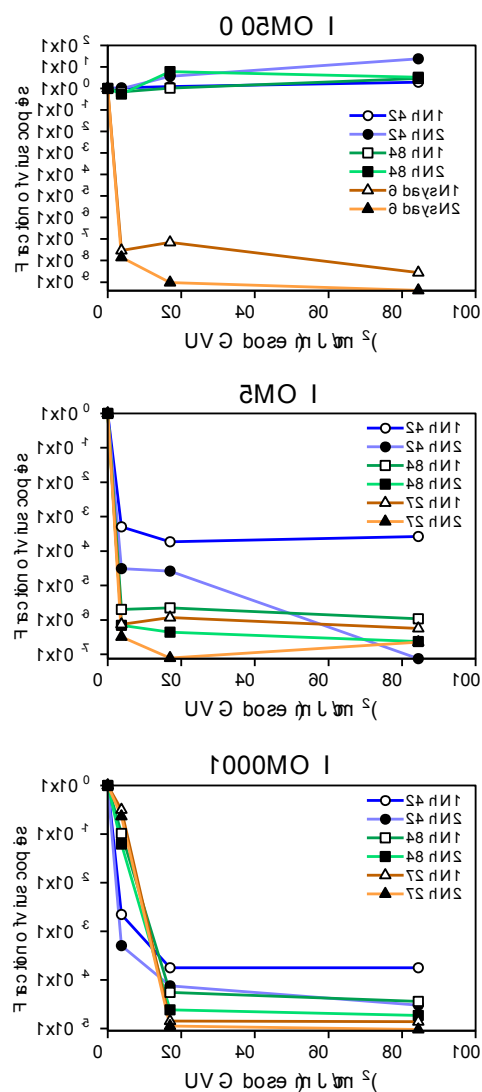


Figure S3. Plots of the measured virus copies normalized at the untreated sample in the different conditions.